Archivum Immunologiae et Therapiae Experimentalis (2020) 68:33
https://doi.org/10.1007/s00005-020-00598-y

ORIGINAL ARTICLE

Astragaloside IV Exerts Anti-tumor Effect on Murine Colorectal Cancer by Re-educating Tumor-Associated Macrophage

Feng Liu[1] · Fang Ran[2] · Hongqin He[1] · Linyun Chen[2]

Received: 12 March 2020 / Accepted: 16 October 2020 / Published online: 23 October 2020

Abstract

Astragaloside IV (AS-IV) has shown anti-tumorigenic properties in certain cancers for its effect of boosting the body's immune system, but its role in colorectal cancer (CRC) remains unclear. In this study, we investigated the therapeutic effect of AS-IV in CRC and explored its underlying mechanism. CT26 colon cancer cells and mouse model by injection of CT26 cells subcutaneously were used as in vitro and in vivo model. M1 and M2 macrophage-associated markers, mRNA and protein expression levels were analyzed after AS-IV treatment. Inflammatory factors and cytokines in the tumors from mouse model were detected. Repolarization effect of AS-IV in vitro on bone-marrow-derived macrophages was also detected. In vitro, AS-IV inhibited the proliferation of CT26 cells and induced cell apoptosis dose-dependently, and significantly reduced M2 macrophages and increased M1 macrophages. In mouse model, it suppressed tumor growth and decreased the production of anti-inflammatory factors such as TGF-β, IL-10 and VEGF-A, while increased the production of pro-inflammatory factors like IFN-γ, IL-12 and TNF-α in tumor. Combination of AS-IV and checkpoint inhibitor aPD-1 exhibited synergistic antitumor effect by inhibiting tumor growth and increasing T cell infiltration. AS-IV could induce M2 macrophages polarization to the M1 phenotype. Its combination with immune checkpoint inhibitors could be expected to become a potential new strategy for the treatment of CRC.

Keywords Colon cancer · Tumor-associated macrophages · Macrophage polarization · Astragaloside IV · Tumor microenvironment

Introduction

Colorectal cancer (CRC) is a common malignant tumor of the digestive system. There are about 1.2 million new cases every year worldwide (Mantovani et al. 2017). It has brought heavy economic and spiritual burdens to people around the world. At present, the treatment of CRC is mainly surgery, chemotherapy, and radiation therapy. There are about 75% of CRC patients who can be diagnosed at an early stage and they can be treated by surgery or/and chemotherapy. But some patients are already in the advanced stage of inoperability at the time of diagnosis and can only get treatment like chemotherapy, radiotherapy and immunotherapy (Ciombor et al. 2015). Thus, it is very urgent to find effective therapeutic strategy for CRC treatment with less side effects for those who are diagnosed at a late stage without the choice of surgery.

Tumor-associated macrophages (TAMs) have become a research hotspot and attracted much attention these days because they play a crucial role in tumor metastasis and therapeutic resistance. TAMs usually accelerate the development of untreated tumors and affect the efficacy of anticancer drugs including checkpoint blockade immunotherapy, and increased numbers of macrophages are associated with poor prognosis (De Palma and Lewis 2013; Mantovani and Allavena 2015; Ruffell and Coussens 2015; Wynn et al. 2013; Zhu et al. 2014). In the tumor microenvironment, macrophages are important immune cells in tumor progression, which depend on different types of tumor and the stage of tumor development (Franklin et al. 2014). In

✉ Linyun Chen
a15511775287@163.com

[1] Department of Anorectal Surgery, Medical College District of CANGZHOU People's Hospital, Intersection of Chongqing Road and Jilin Avenue, Cangzhou 061000, Hebei, China

[2] Division 2 of Neurology, CANGZHOU People's Hospital Headquarters, Qingchi Avenue, Cangzhou 061000, Hebei, China

general, TAMs are considered to promote tumor progression through different mechanisms as there are usually divided into M1 and M2 subgroups and they exert different function. Activated M1 macrophages play an important role in the innate response to fight invading pathogens. Alternately, activated M2 macrophages play a vital role in tumor progression and tissue repair. The tumor-supporting M2 phenotype usually dominates in most tumors. Interest and efforts are thrown into decreasing the number of M2 cells or transforming M2 into M1 cells that can kill the tumor. The latter strategy has drawn great interest in using small molecules to inhibit different receptors, tyrosine kinases, or other important transduction pathways in TAM to induce the transform (Cook et al. 2013; Cuccarese et al. 2017; Pyonteck et al. 2013). Although there are a lots of early preclinical studies and some ongoing clinical trials, the development of new therapies which try to overcome some limitations of present immunotherapy still face many obstacles (Pyonteck et al. 2013). Specific limitations mainly include three aspects. First, there are insufficient understanding of which small molecules most effectively and efficiently affects M2 transformation to M1 phenotype. Second, there are few methods to preferentially deliver small molecules in vivo to TAM. Third, therapeutic efficacy is still suboptimal.

Astragalus membranaceus have the effects of boosting the body's immune system, promoting muscle growth, and diminishing swelling. Astragaloside IV (AS-IV), is one of the main active component of astragalus, and it has a variety of pharmacological activities such as anti-oxidation, anti-inflammation, lowering blood pressure, and improving immunity (Auyeung et al. 2016; Li et al. 2017; Liu et al. 2017). In recent research, AS-IV appears to have powerful antagonistic effects on inflammatory via regulating the inflammatory cytokines and related signaling pathway, and apoptosis-related genes (Li et al. 2020). Studies have shown that astragalus has certain anti-tumor effects, and the combination of astragalus extract and chemotherapy drugs has shown certain advantages in the treatment of CRC (He et al. 2016; Sun et al. 2019; Wang et al. 2018). AS-IV sensitized tumor cells to gefitinib via regulation of SIRT6, suggesting that AS-IV may serve as potential therapeutic approach for lung cancer (Dai et al. 2017). Another recent study showed that AS-IV inhibited the invasion and metastasis of SiHa cervical cancer cells via the TGF-β1-mediated PI3K and MAPK pathways (Zhang et al. 2019). Thus, it is interesting to see if AS-IV has effect on TAMs. In this article, we explored the anti-tumor effect of AS-IV, the main ingredient of astragalus, and whether it exerted the effect on murine CRC by re-educating TAM.

Materials and Methods

Cell Culture

CT26 colon cancer cell line was purchased from The Cell Bank of Type Culture Collection of Chinese Academy of Sciences (Shanghai, China) and were cultured in Dulbecco's modified Eagle's medium (Gibco, USA) supplemented with 10% (Sigma, USA), 100 units/ml penicillin and 100 µg/ml streptomycin at 37 °C in a humidified chamber with 5% CO_2. T cells and NK cells were isolated from the spleen of C57BL6 mouse and cultured in the same medium of CT26 cells. Murine bone marrow-derived macrophages (BMDMs) were isolated according to published literature (Ying et al. 2013). Bone marrow was extracted from the femur and tibia of newborn C57BL/6 mice, dissociated and passed through a 40 µm strainer, and red blood cells were lysed with ammonium chloride (Sigma, USA). The obtained bone marrow cells were inoculated in Iscove's Modified Dulbecco's medium supplemented with 10% heat-inactivated fetal bovine serum, 100 units/ml penicillin, 100 µg/ml streptomycin and 10 ng/ml recombinant mouse macrophage colony-stimulating factor (Sigma, USA) at 37 °C in a humidified chamber with 5% CO_2.

Detection of Cell Viability

After 48 h of treatment with different concentrations of AS-IV (Sigma, Catalog # Y0001171), cell survival was measured by the MTT method. Briefly, cells were seeded in 96-well plates at a concentration of 10,000 cells/well for 24 h. After treated with 10, 50, and 100 nM AS-IV for another 48 h, MTT solution (5 mg/ml) was added for further incubation at 37 °C for 3 h. The spectrophotometric absorbance at 490 nm was measured by a microplate spectrophotometer.

Detection of Apoptotic Cells

Cell apoptosis was quantified by propidium iodide (PI) and Annexin V (AV) staining and detected by a flow cytometry. After treatment with 10, 50, and 100 nM AS-IV for 24 h, CT26 cells were harvested and washed with phosphate-buffered saline (PBS). Cell pellets were stained with AV/PI dilution according to the manufacturer's instruction and analyzed by a flow cytometry (Beckman Coulter, USA).

Flow Cytometry Detection of Percentage of M1 and M2 Macrophages and T Cells

BMDMs were treated with 10 ng/ml recombinant mouse IL-4 (Sigma, USA) for 24 h to induce M2-like polarization state, and then replaced fresh media supplemented with 100 nM AS-IV. Mouse macrophages treated with only IL-4 (10 ng/ml) were used as internal controls for M2-like and M1-like transcription profiles, respectively. After 24 h, cells were collected and stained in phosphate buffered saline containing 0.5% bovine serum albumin (BSA) and 2 mM EDTA with fluorescently labeled antibodies against PE anti-CD206 (eBioscience), PE-cy7 anti-MHC (BioLegend), FITC anti-F4/80 (BioLegend), BV650 anti-CD11b (eBioscience) for 30 min at 4 °C in the dark. Samples were run on an LSR II flow cytometer (BD) and analyzed in FlowJo software to identify M2 macrophages (PE-CD206 + FITC-F4/80) as well as M1 macrophages (PE-Cy7-MHC II + FITC-F4/80).

For in vivo experiments, tumor tissues were collected after experiments. Same weight of tumor tissues was digested with DNAses (0.02 mg/ml), collagenase II (1 mg/ml), and collagenase IV (1 mg/ml) and lightly grinded into single cell suspension by pushing through 300 mesh screens. The following procedure was same as above mentioned. After added labeled antibodies (MHC II, F4/80, CD206), samples were detected with flow cytometry to identify M1 and M2 macrophages. For T cells detection, sample were added eFluor780 anti-CD45.2 (eBioscience), FITC anti-CD4 (BioLegend), PE-CF594 anti-CD8a (BioLegend) for 30 min at 4 °C in the dark, then analyzed by the flow cytometer as mentioned above.

RT-PCR Assay for Genes of M2 Macrophages

For transcriptional analysis, BMDMs were treated with 10 ng/ml of recombinant mouse IL-4 (Sigma, USA) for 24 h to induce M2-like polarization state, and then replaced fresh media supplemented with 100 nM AS-IV. BMDMs treated with only IL-4 (10 ng/ml) were used as internal controls for M2-like and M1-like transcription profiles, respectively. After 24 h, RNA was isolated and analyzed by reverse transcription and qPCR for analysis of arg1 (Mm00475988_m1), mrc1 (Mm01329362_m1), il12 (Mm01288989_m1), and nos2 (Mm00440502_m1). Data are presented as fold change relative to β-actin.

Western Blot Assay for Supramolecules of M2 Macrophages

For protein analysis, BMDMs were treated with 10 ng/ml recombinant mouse IL-4 (Sigma, USA) for 24 h to induce an M2-like polarization state and subsequently changed with fresh media supplemented with 100 nM AS-IV. BMDMs treated only with IL-4 (10 ng/ml) served as internal controls for M2-like and M1-like transcription profiles, respectively. After 24 h, the proteins in the cells were lysed and separated by SDS-PAGE, and then transferred to a PVDF membrane. After blocking with 5% BSA in TBST and 0.1% Tween 20, the primary antibodies of Arg1, Mrc1, IL12, Nos2 and β-actin (Sigma, USA; 1: 1000) were incubated overnight at 4 °C. The secondary antibodies of horseradish peroxidase-conjugated IgG (Sigma, USA; dilution 1:3000) were incubated for 1 h at room temperature. The protein bands on the membrane were detected by enhanced chemiluminescence and analyzed by Image-J software.

Animal Model and Drug Treatment

CT26 colon cancer cells were cultured in RPMI1640 with 10% FBS and digested with 0.5% trypsin when they arrived exponential growth phase. Cells were centrifuged at 800 rpm/min for 5 min and discarded the supernatant. The cell pellets were washed with PBS and resuspended for cells count. After adjusted the final cell concentration to 2×10^7 cells/ml, 100 µl of cell suspension were injected to the axillary fat pad of each BALB/c female mouse (Shanghai SLAC Laboratory Animal Co. Ltd, China). The mice were kept in a clean animal room at 21 ± 2 °C on a 12 h light/dark cycle and with free access to food and water. The animals were divided into four groups as control, AS-IV, aPD1, and AS-IV + aPD1 group. When the tumors grew to 50 mm^3, PBS or drugs (in PBS) were administrated to the mice once every 3 days and totally three times. AS-IV and aPD1 were intraperitoneally administered at 15 mg/kg and 2.5 mg/kg, respectively for AS-IV group and aPD1 group, or both for AS-IV + aPD1 group. Control group mice were given same volume of saline. The InVivoMAb anti-mouse PD-1 (Catalog # BE0146) was bought from Bio X cell. Experiments were approved by the Animal Ethics Committees of CANGZHOU People's Hospital Headquarters and strictly performed according to the NIH guide for the Care and Use of Laboratory Animals.

Tumor Volume and Weight Detection

Tumor growth was measured by digital callipers, and tumor sizes were represented as volume at indicated time points. The tumor volume was detected every 3 days for each mouse and until 22 days after first drug treatment. Then, all the mice were sacrificed and subcutaneous tumor tissues were peeled off and weighed. Tumor volume was measured by Vernier callipers every 3 days and calculated according to the formula of $A \times B^2 \times 0.5$, where A was the maximum diameter of the tumor, B is the shortest diameter.

ELSA Assay for Inflammatory Factor and Cytokines

After treatment, the concentrations of anti-inflammatory factors (TGF-β, IL-10 and VEGF-A) and pro-inflammatory factors (IFN-γ, IL-12, IL12p70 and TNF-α) in tumor tissues were detected by ELISA kits. All the procedures were followed the manufacturer's instructions.

Statistical Analysis

Data were expressed as mean ± SD. SPSS software, Student's *t* test, one- or two-way ANOVA with a post hoc test were used to do statistical analysis. That *p* value was smaller than 0.05 was considered statistically significant.

Results

Effects of AS-IV on the Survival of Murine CRC cell CT26, T Cells, NK Cell and Macrophages

Figure 1a showed the chemical structure of AS-IV. CT26 cells were treated with AS-IV (10, 50, 100 nM) for 48 h and then cell viability was examined by MTT assay. The

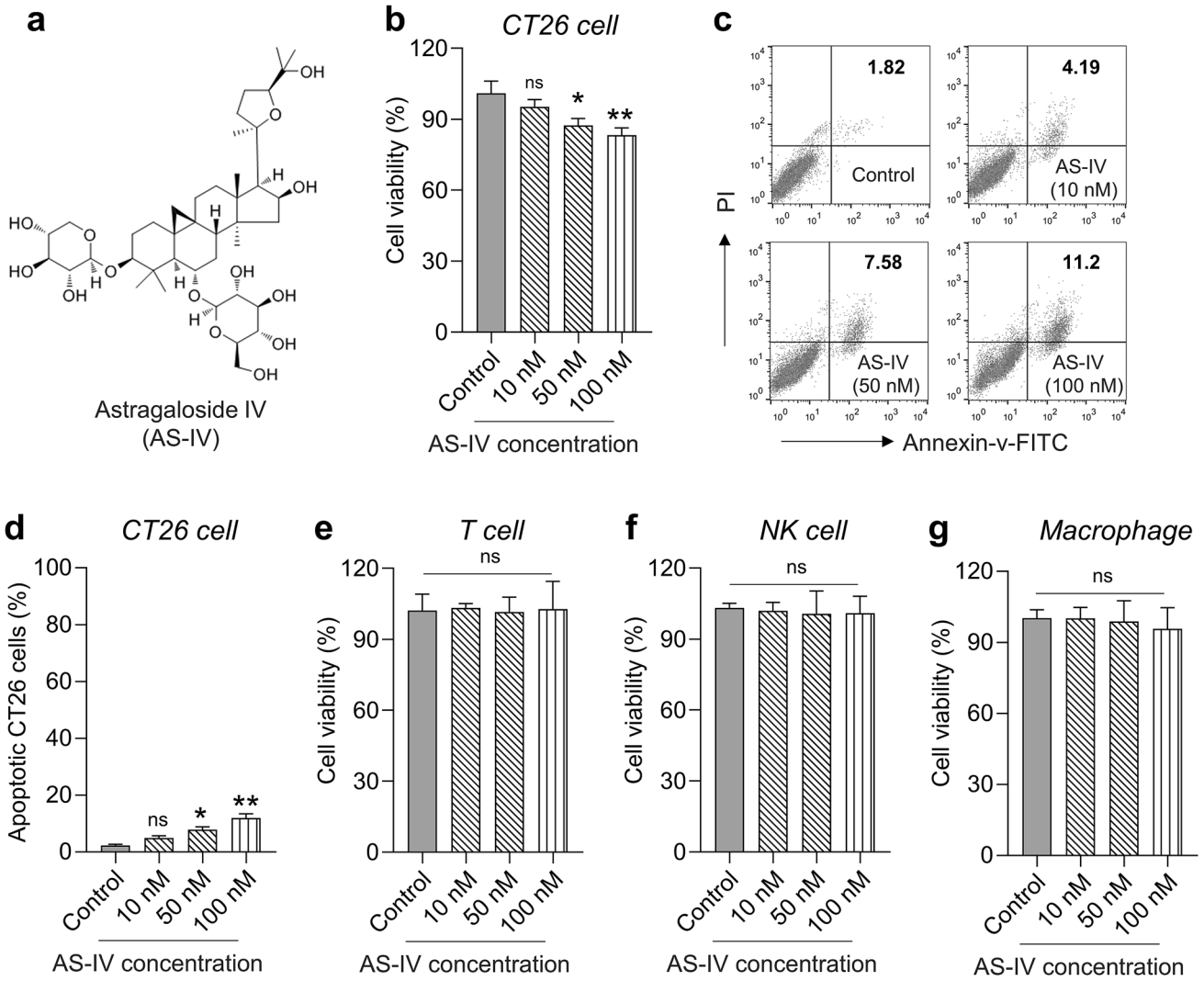

Fig. 1 Effect of Astragaloside IV (AS-IV) on the survival of murine colorectal cancer cell CT26, T cells, NK cell and macrophages. **a** Chemical structure of AS-IV. **b** Viability of CT26 cells after AS-IV treatment. CT26 cells were treated with AS-IV (10, 50, 100 nM) for 48 h and then cell viability was examined by MTT assay. Data are shown as means ± SD, ns, no significant difference, $*p<0.05$, $**p<0.01$ (vs control group). **c** Flow cytometry demonstrating the apoptotic cells. **d** Quantitative analysis of apoptotic cells. CT26 cells were treated as indicated above for 24 h, and then the cell apoptosis was examined by Annexin V/Propidium Iodide apoptosis assay. Data are shown as means ± SD, ns, no significant difference, $*p<0.05$, $**p<0.01$. Viabilities of T cells (**e**), NK cells (**f**) and macrophages (**g**) after treated with different concentrations of AS-IV. T cells and NK cells were isolated from spleen and macrophages were isolated from bone marrow. Data are shown as means ± SD, *ns* no significant difference

results showed that cell viability decreased in a concentration dependent way. When added 100 nM AS-IV, the cell viability decreased significantly (Fig. 1b; $p < 0.01$ vs control group). Flow cytometry demonstrated that apoptotic cells increased as the concentration of AS-IV increased. The apoptotic cells increased when AS-IV increased to 100 nM (Fig. 1c and d; $p < 0.01$ vs control group). MTT experiments also showed that there were no obvious changes in cell viability of T cells (Fig. 1e), NK cells (Fig. 1f) and macrophages (Fig. 1g) after treated with different concentrations of AS-IV, indicating that AS-IV had no toxic effect to these cells in the test concentration.

AS-IV Repolarized Macrophage towards M1 Subtype in Vitro

Figure 2a showed the procedure of murine BMDMs repolarized by 100 nM AS-IV in vitro. BMDMs were incubated with IL-4 for 24 h to induce M2 macrophages, and then treated with 100 nM AS-IV for another 24 h. Cells were collected for analysis and flow cytometry demonstrated the percentages of $CD206^{hi}$ macrophages after 24 h AS-IV treatments greatly decreased (Fig. 2b; $p < 0.001$ vs control group), while the percentages of $MHCII^{hi}$ macrophages increased (Fig. 2c; $p < 0.001$ vs control group). It indicated that AS-IV repolarized macrophage from M2 towards M1 subtype. RT-PCR and western blot results showed that the expression of Arg1 (Fig. 2d) and Mrc1 (Fig. 2e) decreased, while IL12 (Fig. 2f) and NOS2 (Fig. 2g) increased in mRNA level (Fig. 2d–g) and protein level (Fig. 2h–k) in M2 macrophages after treated with 100 nM AS-IV for 24 h ($p < 0.01$ or $p < 0.001$ vs control group).

AS-IV Administration Significantly Inhibited CT26 Tumor Growth and Repolarized Macrophages In Vivo

Figure 3a showed the growth curve of CT26 tumor volume after AS-IV administration. AS-IV (15.0 mg/kg) treatment every 3 days for three times to the mice bearing CT26 tumors of ~ 50 mm^3 inhibited the growth of tumors, showing less tumor volume increase than those mice administration with PBS ($p < 0.01$ vs control at day 22th). The average tumor weight of AS-IV group was less than the control group at the end of experiments (Fig. 3b; $p < 0.01$ vs control). Flow cytometry demonstrated the percentage of $CD11b^{+}F4/80^{+}CD206^{hi}$ M2 macrophages decreased (Fig. 3c and d; $p < 0.01$ vs control) while the percentage of $CD11b^{+}F4/80^{+}MHCII^{hi}$ M1 macrophages increased (Fig. 3e and f; $p < 0.001$ vs control) in tumor tissues with AS-IV administration. The levels of anti-inflammatory factors of TGF-β, IL-10 and VEGF-A in tumor tissues decreased compared to the control group (Fig. 3g; $p < 0.01$ or $p < 0.001$ vs control). On the other hand, the levels of pro-inflammatory factors of IFN-γ, IL-12 and TNF-α in tumor tissues increased compared to the control group (Fig. 3h; $p < 0.05$ or $p < 0.01$ vs control).

Combination of AS-IV and Checkpoint Inhibitor aPD-1 Exhibited Synergistic Antitumor Effects

Combination of AS-IV and checkpoint inhibitor aPD-1 inhibited tumor growth mostly compared to AS-IV or aPD-1 treatment separately in CT26 tumor-bearing Balb/c mice (Fig. 4a; $p < 0.001$). Flow cytometry results showed that the percentage of cytotoxic T cells ($CD8^{+}$ T cells) in the $CD45^{+}$ tumor-infiltrating lymphocytes in tumor tissues from AS-IV + aPD-1 group was higher than those from AS-IV or aPD-1 group (Fig. 4b and c). ELISA results showed that IFN-γ and IL12p70 production in the tumor tissues from AS-IV + aPD-1 group increased more than AS-IV or aPD-1 group (Fig. 4d and e). While TGF-β production in the tumor tissues from AS-IV + aPD-1 group decreased more compared to those from AS-IV or aPD-1 group (Fig. 4f).

Discussion

CRC are one of the most widespread cancers all over the world. The median overall survival of these patients has changed over the past few decades as progress has been made in the development of new therapies. The average survival time of patients with metastatic CRC is 18 months. The main treatment method is still using cytotoxic drugs and irinotecan or oxaliplatin, in combination with 5-FU and calcium folic acid or capecitabine. Targeted therapy significantly improved overall survival in patients with metastatic CRC, ranging 22–29 months (Ciombor et al. 2015). Despite significantly improved overall survival, metastatic CRC patients stop responding to targeted treatments like anti-epidermal growth factor receptor and anti-vascular endothelial growth factor antibodies due to intrinsic and acquired resistance after several months' treatment (Modest et al. 2019). Thus, it remains important to find effective or complementary medicine. In the present study, we investigated the anti-tumor effects of AS-IV, an active compound in the herb of Astragalus membranaceus, via in vitro and in vivo experiments to test if it acts through macrophage polarization.

We first tested the effects of different concentrations of AS-IV on CT26 colon cancer cell line. The experimental results showed that high concentration of AS-IV can inhibit

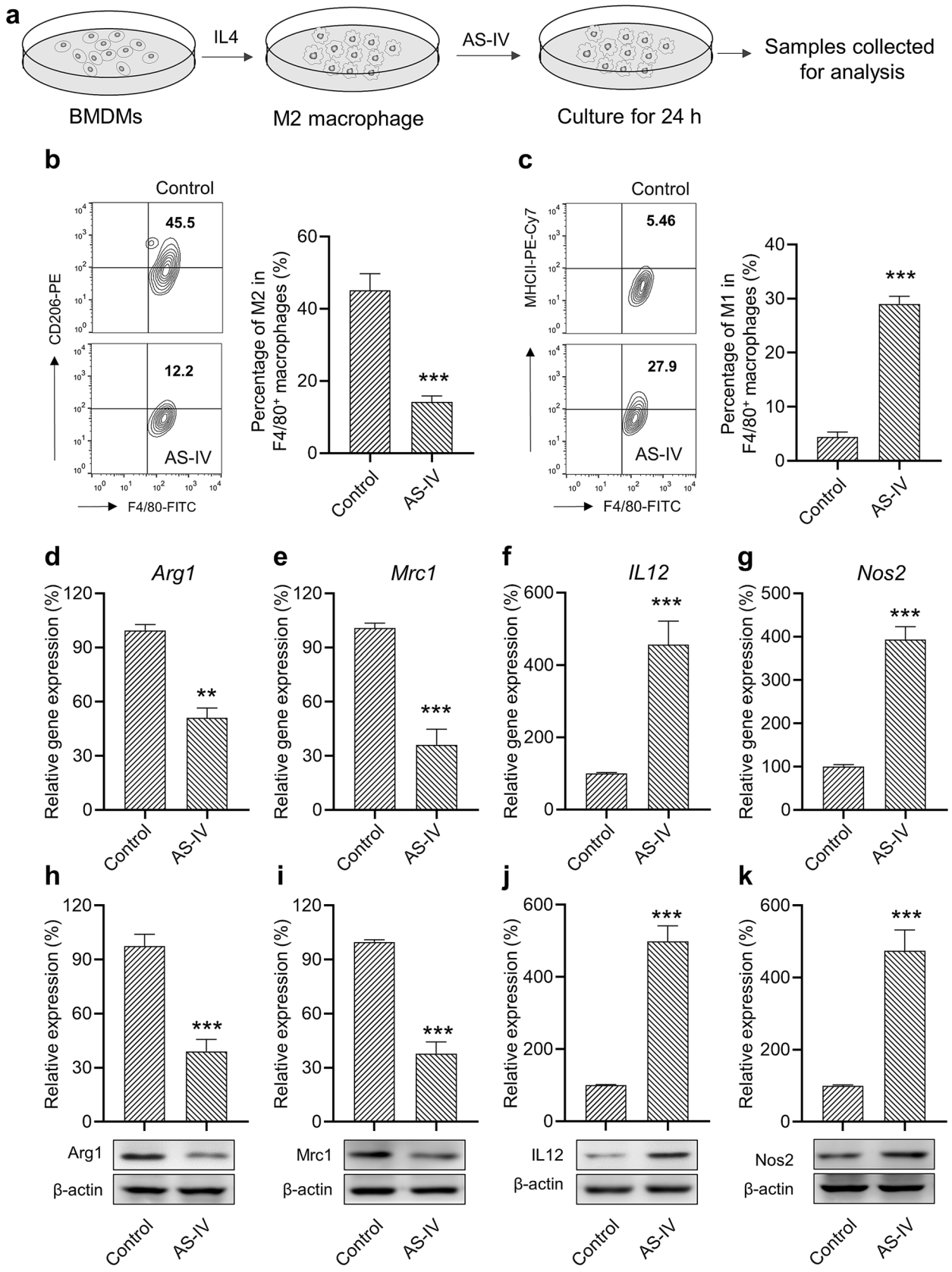
a
IL4
AS-IV
Samples collected for analysis
BMDMs
M2 macrophage
Culture for 24 h
b
Control
45.5
12.2
AS-IV
CD206-PE
F4/80-FITC
Percentage of M2 in F4/80+ macrophages (%)
***
Control
AS-IV
c
Control
5.46
27.9
AS-IV
MHCII-PE-Cy7
F4/80-FITC
Percentage of M1 in F4/80+ macrophages (%)
***
Control
AS-IV
d
Arg1
Relative gene expression (%)
**
Control
AS-IV
e
Mrc1
Relative gene expression (%)
***
Control
AS-IV
f
IL12
Relative gene expression (%)
***
Control
AS-IV
g
Nos2
Relative gene expression (%)
***
Control
AS-IV
h
Relative expression (%)
***
Arg1
β-actin
Control
AS-IV
i
Relative expression (%)
***
Mrc1
β-actin
Control
AS-IV
j
Relative expression (%)
***
IL12
β-actin
Control
AS-IV
k
Relative expression (%)
***
Nos2
β-actin
Control
AS-IV

◂**Fig. 2** AS-IV repolarizes macrophage towards M1 subtype in vitro. **a** Murine bone-marrow-derived macrophages (BMDMs) with IL-4 for 24 h, and then treated with 100 nM AS-IV. Cells were collected for analysis. **b** Flow cytometry demonstrating the percentages of $CD206^{hi}$ macrophages after 24 h AS-IV treatments. **c** Flow cytometry demonstrating the percentages of $MHCII^{hi}$ macrophages after 24 h AS-IV treatments. Data are shown as means ± SD, $***p < 0.001$. **d–g** Expression of Arg1, Mrc1, IL12 and Nos2 in mRNA level in M2 macrophages after treated with 100 nM AS-IV for 24 h. (**h–k**) Expression of Arg1, Mrc1, IL12 and Nos2 in mRNA level in M2 macrophages after treated with 100 nM AS-IV for 24 h. The protein bands on the membrane were detected by enhanced chemiluminescence and analyzed by Image-J software. Data are shown as means ± SD, $**p < 0.01$, $***p < 0.001$ (versus control group)

tumor cell proliferation and induce apoptosis to a certain extent. Subsequently, we tested the effects of AS-IV on the survival of major anti-tumor immune cells like T cells, NK cells and macrophages. Our results showed that even high concentrations of AS-IV had less effects on the viability of these kinds of cells, giving an indication that it will exert less cytotoxicity to immune system.

TAMs, as extremely important cell components and key regulatory cells in the tumor microenvironment, play an important role in tumorigenesis and development, angiogenesis and lymphangiogenesis, invasion, and immune tolerance. It has been verified that M2 macrophages promote tumor growth and M1 macrophages inhibit tumor growth in tumor tissue. Polarizing M2 macrophages into M1 macrophages is an important tumor treatment strategy (Cully 2018; Liu et al. 2015; Mantovani et al. 2017; Ni et al. 2015). Therefore, we further examined the effect of AS-IV on the polarization of macrophages. We used murine BMDMs to detect repolarization effect of AS-IV in vitro. BMDMs were incubated with IL-4 for 24 h to induce M2 macrophages, and then treated with 100 nM AS-IV for another 24 h. Flow cytometry analysis showed that the surface marker CD206 in M2 macrophages was significantly reduced, and the expression of M1 surface marker MHCII was significantly increased when treated with AS-IV. Simultaneously, the expression levels of M2-related genes such as Arg1 and Mrc1 and corresponding proteins were significantly downregulated, while the expression levels of M1-related genes such as IL12 and Nos2 and corresponding proteins were significantly increased after treatment of AS-IV to M2 macrophages from BMDM induced by IL-4. These results indicated that AS-IV can effectively induce M2 cells to M1 cell repolarization. Xu et al. reported that AS-IV reduced the invasion, migration, and angiogenesis of lung cancer by modulating macrophage polarization partially through the AMPK signaling pathway (Xu et al. 2018). Our results also verified that AS-IV induced M2 macrophages polarization to the M1 phenotype.

Next, we built a murine colorectal cancer CT26 subcutaneous model to test AS-IV antitumor effect in vivo. AS-IV (15.0 mg/kg) treatment every 3 days for three times to the mice bearing CT26 tumors of ~ 50 mm^3 inhibited the growth of tumors, showing less tumor volume increase and average tumor weight at the end of experiments than those mice administration with PBS. The results showed that AS-IV had a certain antitumor effect, and at the same time, it can polarize macrophages in vivo showing that the percentage of $CD11b^{+}F4/80^{+}CD206^{hi}$ M2 macrophages decreased while the percentage of $CD11b^{+}F4/80^{+}MHCII^{hi}$ M1 macrophages increased in tumor tissue by AS-IV treatment. Previous study showed that AS-IV administration significantly reduced cell growth and induced a notable cell cycle arrest in G0/G1 phase of CRC cell lines in a dose dependent manner. In addition, expression levels of B7-H3 protein and key G0/G1 cell cycle checkpoint proteins (e.g. cyclin D1 and CDK4) were predominantly decreased in response to AS-IV treatment (Wang et al. 2018). Our results are consistent with this study that AS-IV is a promising anti-cancer drug in CRC.

Immunotherapy and treatment strategies aimed at reducing the proportion of M2 macrophages or transforming M2 macrophages into M1 macrophages that can inhibit tumor growth and metastasis (Ostuni et al. 2015; Sica et al. 2006). This study further supported this conclusion. In our study, AS-IV significantly inhibited M2 polarization in vivo and in vitro, and significantly affected tumor development. It has been verified that inflammation is one of the causes of carcinogenesis, and macrophage polarization is the entry point for the microenvironment of inflammation (Qian and Pollard 2010). Cytokines often have pro-inflammatory or anti-inflammatory effects, and the balance between the two determines the direction of the inflammatory response. Our study revealed that AS-IV clearly decreased the expression of anti-inflammatory factors such as TGF-β, IL-10 and VEGF-A, and increased the expression of pro-inflammatory factors like IFN-γ, IL-12 and TNF-α in tumor tissues after treatment. These results showed that AS-IV regulated microenvironment of inflammation and M2 macrophage polarization.

Studies have shown that M2 macrophages can reverse the immunosuppressive microenvironment of tumors and increase the infiltration of cytotoxic T cells after polarizing to M1. Thus, we further tested AS-IV combined with PD-1 antibody for treatment. The experimental results show that the combination treatment group can inhibit tumor growth and increase T cell infiltration much better than AS-IV

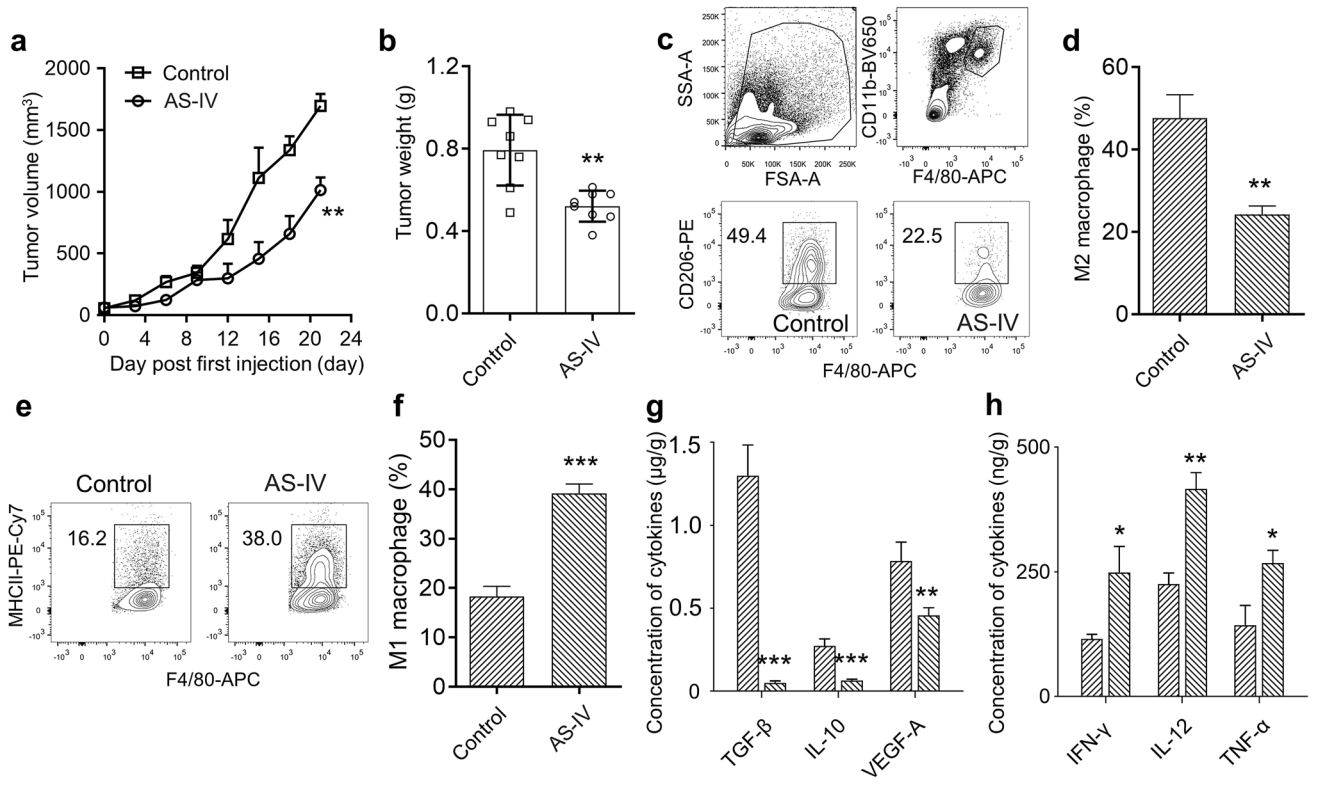

Fig. 3 AS-IV administration significantly inhibit CT26 tumor growth and repolarize macrophages in vivo. **a** Growth of CT26 tumor after AS-IV administration. Mice bearing CT26 tumors of ~ 50 mm^3 received PBS or AS-IV every 3 days for three times, the administration dosage of AS-IV was 15.0 mg/kg, respectively. $^{**}p < 0.01$. **b** Tumor weights of different group at the end of treatments. $^{**}p < 0.01$. Flow cytometry demonstrates the ratios of $CD11b^{+}F4/80^{+}CD206^{hi}$ M2 macrophages (**c**) and $CD11b^{+}F4/80^{+}MHCII^{hi}$ M1 macrophages (**e**) at the end of treatments. Bar graph shows the percentage of M2 macrophages (**d**) and M1 macrophages (**f**) in tumor tissues. Data are shown as means ± SD ($n = 5$). $^{**}p < 0.01$, $^{***}p < 0.001$. **g** Levels of anti-inflammatory factors (TGF-β, IL-10 and VEGF-A) in tumor tissues. **h** Levels of pro-inflammatory factors (IFN-γ, IL-12 and TNF-α) in tumor tissues. Data are shown as means ± SD ($n = 5$). $^{*}p < 0.05$, $^{**}p < 0.01$, $^{***}p < 0.001$

alone. At the same time, the expression of immunosuppression-related cytokines (such as TGF-β) in the combination treatment was relatively low, while immune activation and tumor killing related cytokines (such as IL12p70 and IFN-γ) were significantly up-regulated. This study showed that AS-IV had the ability to regulate the polarization of macrophages, and its combination with immune checkpoint inhibitors is expected to become a new strategy for the treatment of CRC. We have still some limitations in this article that we should use more cell lines and animal models to avoid model-dependency and do further experiments to clarify the downstream cellular targets and pathways for AS-IV.

In summary, we reported here that AS-IV, an active compound in the herb of Astragalus membranaceus, could inhibit tumor cell proliferation and induce cell apoptosis. It exerted the anti-tumor effects in vitro and in vivo through effect on macrophage by promoting M2 macrophage polarization to the M1 phenotype. Combination of AS-IV and checkpoint inhibitor aPD-1 exhibited synergistic antitumor effect by inhibiting tumor growth and increasing T cell infiltration. Our study indicated that AS-IV has the ability to regulate

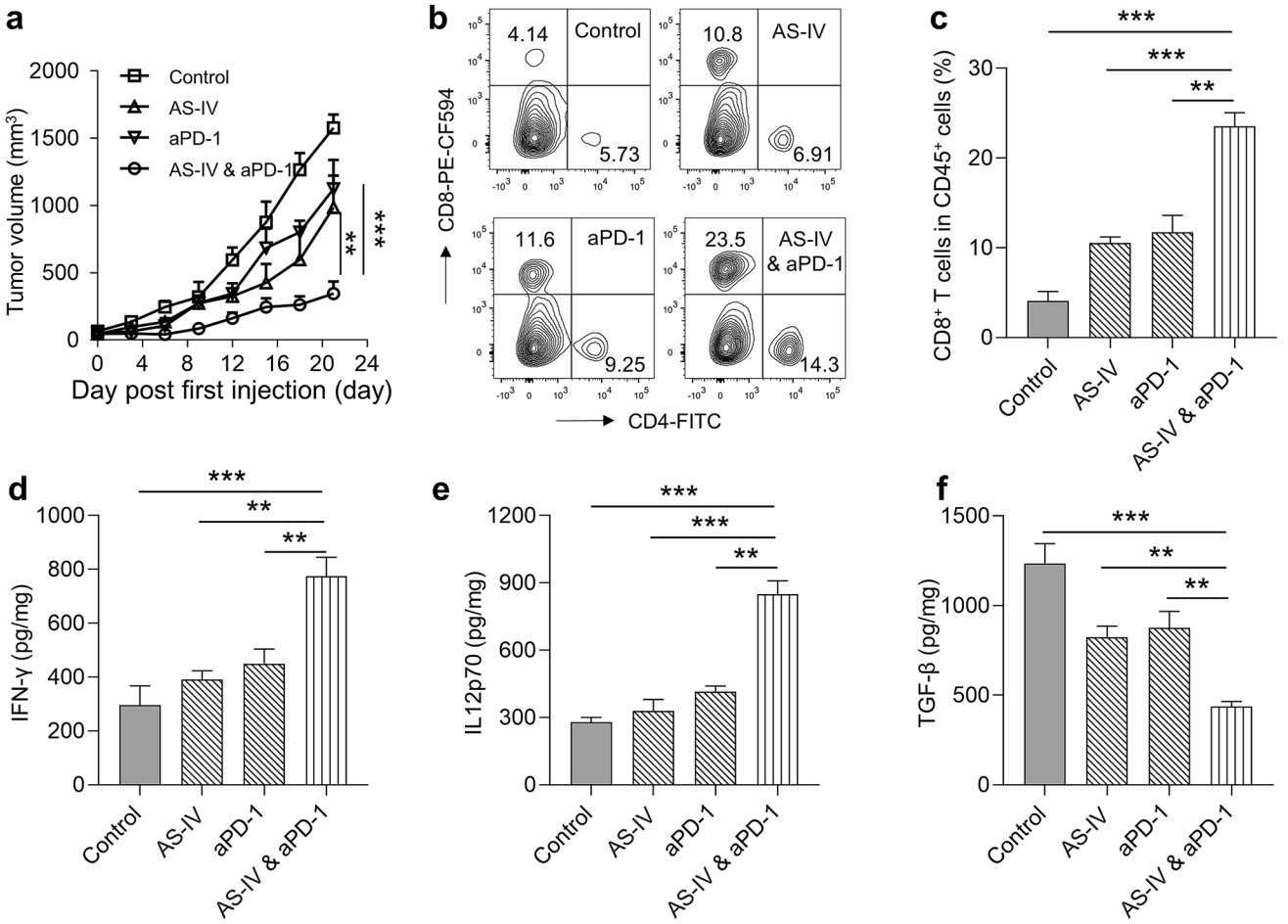

Fig. 4 Combination of AS-IV and checkpoint inhibitor aPD-1 exhibit synergistic antitumor effect. **a** Inhibition of tumor growth by various treatments in CT26 tumor-bearing Balb/c mice ($n=8$). Mice bearing CT26 tumors of ~50 mm^3 received PBS, AS-IV, aPD-1 or combination of AS-IV and aPD-1 every 3 days for three times, the administration dosage of AS-IV and aPD-1 were 15.0 mg/kg (i.v.) and 2.5 mg/kg (i.v.), respectively. $^{**}p<0.01$, $^{***}p<0.001$. **b** Flow cytometry gating of cytotoxic T cells ($CD8^+$ T cells) in the $CD45^+$ tumor-infiltrating lymphocytes in tumor tissues from mice receiving indicated treatment. **c** Percentages of $CD8^+$ T cells in $CD45^+$ cells based on the analysis of flow cytometric examination. ELISA results of cytokines production (**d** FN-γ, **e** IL12p70, **f** TGF-β) in the tumors from mice receiving indicated treatments. Data represent means ± SD. $n=5$, $^{**}p<0.01$, $^{***}p<0.001$

the polarization of macrophages, and its combination with immune checkpoint inhibitors was expected to become a potential new strategy for the treatment of CRC.

Funding None.

Compliance with Ethical Standards

Conflict of Interest The authors declare that they have no conflict of interest.

References

Auyeung KK, Han QB, Ko JK (2016) Astragalus membranaceus: a review of its protection against inflammation and gastrointestinal cancers. Am J Chin Med 44:1–22. https://doi.org/10.1142/S0192415X16500014

Ciombor KK, Wu C, Goldberg RM (2015) Recent therapeutic advances in the treatment of colorectal cancer. Annu Rev Med 66:83–95. https://doi.org/10.1146/annurev-med-051513-102539

Cook RS, Jacobsen KM, Wofford AM et al (2013) MerTK inhibition in tumor leukocytes decreases tumor growth and metastasis. J Clin Invest 123:3231–3242. https://doi.org/10.1172/JCI67655

Cuccarese MF, Dubach JM, Pfirschke C et al (2017) Heterogeneity of macrophage infiltration and therapeutic response in lung carcinoma revealed by 3D organ imaging. Nat Commun 8:14293. https://doi.org/10.1038/ncomms14293

Cully M (2018) Cancer: re-educating tumour-associated macrophages with nanoparticles. Nat Rev Drug Discov 17:468. https://doi.org/10.1038/nrd.2018.102

Dai PC, Liu DL, Zhang L et al (2017) Astragaloside IV sensitizes non-small cell lung cancer cells to gefitinib potentially via regulation of SIRT6. Tumour Biol 39:1010428317697555. https://doi.org/10.1177/1010428317697555

De Palma M, Lewis CE (2013) Macrophage regulation of tumor responses to anticancer therapies. Cancer Cell 23:277–286. https://doi.org/10.1016/j.ccr.2013.02.013

Franklin RA, Liao W, Sarkar A et al (2014) The cellular and molecular origin of tumor-associated macrophages. Science 344:921–925. https://doi.org/10.1126/science.1252510

He CS, Liu YC, Xu ZP et al (2016) Astragaloside IV enhances cisplatin chemosensitivity in non-small cell lung cancer cells through inhibition of B7–H3. Cell Physiol Biochem 40:1221–1229. https://doi.org/10.1159/000453175

Li L, Hou X, Xu R et al (2017) Research review on the pharmacological effects of astragaloside IV. Fundam Clin Pharmacol 31:17–36. https://doi.org/10.1111/fcp.12232

Li S, Yi Sun Y, Huang J et al (2020) Anti-tumor effects and mechanisms of Astragalus membranaceus (AM) and its specific immunopotentiation: status and prospect. J Ethnopharmacol 258:112797. https://doi.org/10.1016/j.jep.2020.112797

Liu G, Bi Y, Xue L et al (2015) Dendritic cell SIRT1-HIF1alpha axis programs the differentiation of CD4+ T cells through IL-12 and TGF-beta1. Proc Natl Acad Sci USA 112:E957-965. https://doi.org/10.1073/pnas.1420419112

Liu P, Zhao H, Luo Y (2017) Anti-aging implications of astragalus membranaceus (Huangqi): a well-known Chinese tonic. Aging Dis 8:868–886. https://doi.org/10.14336/AD.2017.0816

Mantovani A, Allavena P (2015) The interaction of anticancer therapies with tumor-associated macrophages. J Exp Med 212:435–445. https://doi.org/10.1084/jem.20150295

Mantovani A, Marchesi F, Malesci A et al (2017) Tumour-associated macrophages as treatment targets in oncology. Nat Rev Clin Oncol 14:399–416. https://doi.org/10.1038/nrclinonc.2016.217

Modest DP, Pant S, Sartore-Bianchi A (2019) Treatment sequencing in metastatic colorectal cancer. Eur J Cancer 109:70–83. https://doi.org/10.1016/j.ejca.2018.12.019

Ni YH, Ding L, Huang XF et al (2015) Microlocalization of CD68+ tumor-associated macrophages in tumor stroma correlated with poor clinical outcomes in oral squamous cell carcinoma patients. Tumour Biol 36:5291–5298. https://doi.org/10.1007/s13277-015-3189-5

Ostuni R, Kratochvill F, Murray PJ et al (2015) Macrophages and cancer: from mechanisms to therapeutic implications. Trends Immunol 36:229–239. https://doi.org/10.1016/j.it.2015.02.004

Pyonteck SM, Akkari L, Schuhmacher AJ et al (2013) CSF-1R inhibition alters macrophage polarization and blocks glioma progression. Nat Med 19:1264–1272. https://doi.org/10.1038/nm.3337

Qian BZ, Pollard JW (2010) Macrophage diversity enhances tumor progression and metastasis. Cell 141:39–51. https://doi.org/10.1016/j.cell.2010.03.014

Ruffell B, Coussens LM (2015) Macrophages and therapeutic resistance in cancer. Cancer Cell 27:462–472. https://doi.org/10.1016/j.ccell.2015.02.015

Sica A, Schioppa T, Mantovani A et al (2006) Tumour-associated macrophages are a distinct M2 polarised population promoting tumour progression: potential targets of anti-cancer therapy. Eur J Cancer 42:717–727. https://doi.org/10.1016/j.ejca.2006.01.003

Sun P, Liu Y, Wang Q et al (2019) Astragaloside IV inhibits human colorectal cancer cell growth. Front Biosci 24:597–606

Wang S, Mou J, Cui L et al (2018) Astragaloside IV inhibits cell proliferation of colorectal cancer cell lines through down-regulation of B7–H3. Biomed Pharmacother 102:1037–1044. https://doi.org/10.1016/j.biopha.2018.03.127

Wynn TA, Chawla A, Pollard JW (2013) Macrophage biology in development, homeostasis and disease. Nature 496:445–455. https://doi.org/10.1038/nature12034

Xu F, Cui WQ, Wei Y et al (2018) Astragaloside IV inhibits lung cancer progression and metastasis by modulating macrophage polarization through AMPK signaling. J Exp Clin Cancer Res 37:207. https://doi.org/10.1186/s13046-018-0878-0

Ying W, Cheruku PS, Bazer FW et al (2013) Investigation of macrophage polarization using bone marrow derived macrophages. J Vis Exp 76:50323. https://doi.org/10.3791/50323

Zhang L, Zhou J, Qin X et al (2019) Astragaloside IV inhibits the invasion and metastasis of SiHa cervical cancer cells via the TGFbeta-1mediated PI3K and MAPK pathways. Oncol Rep 41:2975–2986. https://doi.org/10.3892/or.2019.7062

Zhu Y, Knolhoff BL, Meyer MA et al (2014) CSF1/CSF1R blockade reprograms tumor-infiltrating macrophages and improves response to T-cell checkpoint immunotherapy in pancreatic cancer models. Cancer Res 74:5057–5069. https://doi.org/10.1158/0008-5472.CAN-13-3723